Journal of Chromatography B 1144 (2020) 122098

Contents lists available at ScienceDirect

Journal of Chromatography B

journal homepage: www.elsevier.com/locate/jchromb

Bioanalytical assay for the new-generation ROS1/TRK/ALK inhibitor repotrectinib in mouse plasma and tissue homogenate using liquid chromatography-tandem mass spectrometry

Wenlong Li[a,b,*], Nikoletta Perpinioti[a], Alfred H. Schinkel[b], Jos H. Beijnen[a,c,d], Rolf W. Sparidans[e]

[a] Utrecht University, Faculty of Science, Department of Pharmaceutical Sciences, Division of Pharmacoepidemiology & Clinical Pharmacology, Universiteitsweg 99, 3584 CG Utrecht, the Netherlands
[b] The Netherlands Cancer Institute, Division of Pharmacology, Plesmanlaan 121, 1066 CX Amsterdam, the Netherlands
[c] The Netherlands Cancer Institute, Department of Clinical Pharmacology, Plesmanlaan 121, 1066 CX Amsterdam, the Netherlands
[d] The Netherlands Cancer Institute, Department of Pharmacy & Pharmacology, Louwesweg 6, 1066 EC Amsterdam, the Netherlands
[e] Utrecht University, Faculty of Science, Department of Pharmaceutical Sciences, Division Pharmacology, Universiteitsweg 99, 3584 CG Utrecht, the Netherlands

ARTICLE INFO

Keywords:
Repotrectinib
LC-MS/MS
Mouse plasma
Mouse tissue
Pharmacokinetics
ROS1/TRK/ALK inhibitor

ABSTRACT

Repotrectinib, a next-generation ROS1/TRK/ALK tyrosine kinase inhibitor, overcomes resistance due to acquired solvent-front mutations involving ROS1, NTRK1-3, and ALK. A bioanalytical assay for quantification of repotrectinib in mouse plasma and seven tissue-related matrices (brain, liver, spleen, kidney, small intestinal tissue, small intestinal content, and testis homogenates) was developed and validated using liquid chromatography with tandem mass spectrometric detection in a high-throughput 96-well format. Protein precipitation was performed by adding acetonitrile, also containing the internal standard axitinib, to 10-µl samples for all matrices. Chromatographic separation of analytes was done on an ACQUITY UPLC® BEH C18 column by gradient elution using ammonium hydroxide in water and methanol. Compounds were monitored with positive electrospray ionization using a triple quadruple mass spectrometer in selected reaction monitoring mode. The method was successfully validated in the 1–1000 ng/ml calibration range. Precisions (intra- and interday) were in the range of 1.3–8.7% and accuracies were in between 90.5% and 107.3% for all levels in all matrices. The developed method was successfully applied to investigate the plasma pharmacokinetics and tissue accumulation of repotrectinib in wild-type mice.

1. Introduction

ROS1 (c-ros-oncogene) rearrangement was first found in a glioblastoma cell line, and since then it has been connected to several other malignancies, such as inflammatory myofibroblastic tumor, ovarian cancer, gastric cancer, colorectal cancer and non-small cell lung cancer (NSCLC) [1]. Activating gene rearrangements in anaplastic lymphoma kinase (ALK) have been identified as oncogenic drivers in 3–7% of patients with NSCLC and other cancers [2]. ROS1 and ALK share extensive amino acid homology, especially in their kinase domain [3]. Since ROS1 and ALK rearrangements present promising molecular targets for treatment, several ROS1 and/or ALK inhibitors have been developed [4]. Crizotinib was the first ALK/ROS1 inhibitor approved by the FDA in 2011. More recently, the neurotrophic tropomysin receptor kinase (NTRK) gene fusions involving either NTRK1, NTRK2, or NTRK3 (encoding the neurotrophin receptors TRKA, TRKB and TRKC, respectively) have been shown to be oncogenic drivers in many adult and pediatric malignancies [5–7]. Larotrectinib and entrectinib have been approved by the FDA for the treatment of solid tumors with TRK rearrangement regardless of age and tumor origin in 2018 and 2019, respectively. Despite the promising clinical activity of earlier-generation tyrosine kinase inhibitors (TKIs), resistance invariably develops.

Abbreviations: ALK, anaplastic lymphoma kinase; LC – MS/MS, liquid chromatography-tandem mass spectrometry; LLOQ, lower limit of quantification; NSCLC, non-small cell lung cancer; NTRK, neurotrophic tropomyosin receptor kinase; QC, quality control; R^2, coefficient of determination; ROS1, c-ros-oncogene; SD, standard deviation; SRM, selected reaction monitoring; TKI, tyrosine kinase inhibitor; TRK, tropomyosin receptor kinase

* Corresponding author at: Utrecht University, Faculty of Science, Department of Pharmaceutical Sciences, Division of Pharmacoepidemiology & Clinical Pharmacology, Universiteitsweg 99, 3584 CG Utrecht, the Netherlands.
E-mail addresses: w.li@nki.nl (W. Li), nperpinioti@gmail.com (N. Perpinioti), a.schinkel@nki.nl (A.H. Schinkel), j.beijnen@nki.nl (J.H. Beijnen), r.w.sparidans@uu.nl (R.W. Sparidans).

https://doi.org/10.1016/j.jchromb.2020.122098
Received 14 February 2020; Received in revised form 27 March 2020; Accepted 30 March 2020
Available online 01 April 2020

Repotrectinib (TPX-0005), a new-generation ROS1/TRK/ALK tyrosine kinase inhibitor, was designed to efficiently bind with the active kinase conformation and avoid steric interference from a variety of clinically resistant mutations, especially the solvent-front and gatekeeper mutations of ROS1, TRK and ALK kinases [8]. In line with this, repotrectinib has displayed highly potent antiproliferative activity against wild-type fusion proteins and their solvent front mutations involving ROS1, TRK and ALK in cellular inhibitory assays and xenograft models in multiple preclinical models [8]. Moreover, in patients with ROS1- or NTRK3-rearranged tumors that harbor resistant solvent front mutations, repotrectinib showed prominsing antitumor activity [8]. Currently, repotrectinib is under investigation in Phase-I/II clinical trials in patients with advanced solid tumors harboring ROS1, TRK, and ALK rearrangements (NCT03093116; NCT04094610).

To date, very limited information is publicly available about bioanalytical studies for repotrectinib. A sensitive and robust bioanalytical assay for this drug will be indispensable for future preclinical and clinical studies. Therefore, in the present study a straightforward LC-MS/MS method in a high-throughput 96-well format was developed and validated for the quantitative analysis of repotrectnib in mouse plasma and homogenates of seven different tissue-related matrices: brain, kidney, liver, small intestinal tissue, small intestinal content, spleen, and testis, to support preclinical studies with this drug.

2. Material and methods

2.1. Chemicals and reagents

Repotrectinib was supplied by TargetMol (Wellesley Hills, MA, USA). Axitinib hydrochloric acid (> 99%), used as internal standard (IS), was purchased from Carbosynth (Compton, Berkshire, UK) under its previous name Sequoia Research Products (Pangbourne, UK). Methanol of HPLC quality, acetonitrile of gradient quality, and water of ULC-MS quality (for preparation of eluent) were provided by Biosolve (Valkenswaard, The Netherlands). Analytical grade ammonium hydroxide was acquired from Sigma-Aldrich (Steinheim, Germany). Water purified by reversed osmosis on a multi-laboratory scale was used for other purposes. Human lithium heparin plasma (mixed gender) and pooled CD-1 mouse lithium heparin plasma (female) were from Sera Laboratories (Haywards Heath, West Sussex, UK).

2.2. Tissue homogenization

The whole brain, kidney, liver, small intestinal tissue (SI), small intestinal content (SIC), spleen, and testis were weighed and homogenized with 1, 2, 3, 3, 2, 1, and 1 ml of ice-cold 2% (w/v) bovine serum albumin in water, respectively, using the FastPrep-24™ 5G instrument (M.P. Biomedicals, Santa Ana, CA, USA) for 1 min.

2.3. Analytical instruments

The Shimadzu (Kyoto, Japan) Nexera X2 chromatographic system equipped with a Sil30-ACmp autosampler, a CTO-20 AC column oven, a DGU-20A5R degasser, and two LC30-AD pumps was used. The triple quadrupole mass spectrometer AB SCIEX QTRAP® 5500 (Ontario, Canada), equipped with an inlet valve and a Turbo V™ TurboIonSpray® probe, was adopted for detection. Analyst 1.6.2. (Sciex) software was applied for collecting data and controlling the LC system and mass spectrometer. All LC-MS/MS data were processed and analyzed using the MultiQuant 3.0.1.

2.4. LC-MS/MS conditions

An ACQUITY UPLC® BEH C18 column (30 × 2.1 mm, d_p = 1.7 µm, Waters, Milford, USA) protected by the corresponding VanGuard pre-column (5 × 2.1 mm, d_p = 1.7 µm, Waters) was applied for partial loop injections (1 µl) at 40 °C to separate repotrectinib and IS. The sample rack containing deep 96-well plates was maintained at 4 °C in the autosampler. The gradient elution, using (A) 0.1% (v/v) ammonium hydroxide in water and (B) methanol, was performed at a flow rate of 0.5 ml/min. After injection, the percentage of methanol was linearly increased from 45 to 70% in 1.5 min, followed by flushing at 100% methanol for 0.2 min. Finally, the column was reconditioned at initial conditions for 0.3 min before starting the new injection procedure (ca. 0.5 min). The eluent was transferred to the electrospray by the divert valve from 0.6 to 1.8 min.

Optimum electrospray and selective reaction monitoring (SRM) conditions were obtained by ramping individual parameters during infusion of 100 ng/ml repotrectinib (and axitinib separately) at 10 µl/min in methanol/0.1% ammonium hydroxide in water (50/50; v/v). Settings with highest responses were used for monitoring both compounds: collision gas (CAD), medium; curtain gas (CUR), 10 psi; temperature (TEM), 700 °C; ion source gas 1 (GS1), 60 psi; ion source gas 2 (GS2), 50 psi; entrance potential (EP), 12 V; ion-spray voltage (IS), 5500 V. Mass transitions were monitored at 150 ms dwell times and unit mass resolutions, their individual parameters are listed in Table 1.

Table 1
MS/MS parameters for SRM monitoring of repotrectinib and the internal standard axitinib.

Compound	*m/z* Q1	*m/z* Q3	DP (V)	CE (V)	CXP (V)
Repotrectinib	356.1	106.0	121	73	12
Axitinib	387.1	356.0	171	29	16

DP: declustering potential, CE: collision energy, CXP: collision cell exit potential.

2.5. Stock and working solution

The stock solutions of repotrectinib were prepared in methanol at concentrations of 0.5 and 1 mg/ml. The stock solution of 1 mg/ml axitinib was prepared in methanol. Working solutions of repotrectinib were obtained by diluting the stock solution 10- or 20-fold with water/methanol (1/1; v/v) to 50 µg/ml for calibration and quality control (QC) samples, respectively. An axitinib working solution was prepared by diluting the stock solution 100-fold with water/methanol (1/1; v/v) to 10 µg/ml, which was further diluted 250-fold in acetonitrile to get 40 ng/ml axitinib solution for extraction. All the solutions were stored at −30 °C.

2.6. Calibration standards and quality control samples

The highest calibration sample at 1000 ng/ml was made by diluting the 50 µg/ml repotrectinib working solution with blank mouse plasma in polypropylene tubes, stored at −30 °C until further use. Additional calibration samples were produced daily by diluting highest calibration solution to 500, 100, 50, 10, 5, 2, and 1 ng/ml with blank mouse plasma. Quality control (QC) samples were prepared at 750 (high), 50 (medium), 2.5 (low), and 1 ng/ml (lower limit of quantification (LLOQ)) in mouse plasma from a second 50 µg/ml QC working solution by sequential dilution. Dilution integrity sample at 4000 ng/ml was prepared by diluting this 50 µg/ml QC working solution with blank mouse plasma. QC samples at 50 ng/ml (medium) were also prepared in pooled mouse tissue homogenates of brain, liver, spleen, kidney, small intestinal tissue, small intestinal content, and testis. These QCs were also stored at −30 °C until further use.

2.7. Sample preparation

Ten µl plasma or tissue homogenate was pipetted into a well in a 200 µl polypropylene 96-well plate with conical bottom, where 20 µl of

40 ng/ml axitinib in acetonitrile was added. The 96-well plate was closed with a silicone mat and vigorously vortex mixed for a few seconds to precipitate proteins. Centrifugation at 2643*g* for 5 min at 20 °C resulted in a clear supernatant of which 20 µl was transferred into a 96-deep 1-ml well plate with a round bottom. After adding 200 µl of 25% (v/v) methanol in water, samples were mixed gently but thoroughly by manual shaking. The prepared plate was placed in the autosampler rack for injection of 1 µl of the diluted sample extracts.

2.8. Bioanalytical method validation

The quantification range of 1–1000 ng/ml was validated following international guidelines (FDA and EMA) with full validation for mouse plasma and partial validation for seven tissue homogenates [9,10]. Validation for tissue homogenates was therefore limited to one level for precision and accuracy, selectivity experiments and relative matrix effect with 4 individual blank homogenates for each tissue, and short-term (bench-top) stability and incurred sample reanalysis for 36 homogenates of the repotrectinib pharmacokinetic study.

2.8.1. Selectivity

The selectivity of this assay was studied for six individual mouse plasma and 28 tissue homogenates (4 individual homogenates for each tissue). Each sample was analyzed as double blank (no analyte, no IS), and as LLOQ spiked sample (1 ng/ml repotrectinib).

2.8.2. Recovery and matrix effect

Recoveries for matrix effect and extraction were investigated at three QC levels (high, medium, low) in mouse plasma. In addition to original plasma QC samples, samples were prepared in methanol at 67.7% of the original levels, reaching at 500, 33.3, and 1.67 ng/ml for high-, medium-, and low-QC level, respectively. Three types of samples were prepared (n = 6 for each level). Plasma QC samples were processed using the original procedure (A). Methanolic QC samples (10 µl) were added to blank extracts (20 µl, containing IS) and diluted with 190 µl 25% methanol in water (v/v) (B). And at last methanolic QC samples (10 µl) were diluted with 10 µl acetonitrile and 200 µl water/methanol (1/1; v/v) (C). Extraction recovery was calculated from ratio A/B, matrix effects from B/C.

Relative matrix effects were assessed for six individual mouse plasma and 28 tissue homogenate samples used in the selectivity determinations. The blank extracts were supplemented with drug at the high and low level, respectively, and mixed with the IS. The relative matrix effect was calculated by comparison with matrix-free reference solutions containing both compounds at the same concentrations.

2.8.3. Calibration curve

All plasma calibration samples were prepared in duplicate for each daily calibration together with additional blank (no analyte) and double blank (no analyte and no axitinib) control samples. The calibration curve was constructed using weighted quadratic least squares regression with $1/x^2$ (x is the concentration of repotrectinib) as the weighting factor and data were calculated from the peak area of analyte relative to the IS. For the axitinib IS combined peak areas of both non-separated isomers were used. Plasma calibration was used as surrogate matrix for analysis of tissue samples as well.

2.8.4. Precision and accuracy

Assay performance (within- and between-day) was assessed at four levels for plasma samples (Table 2) and one level for each of the seven tissue homogenates (Table 3). Precision and accuracy were determined in three separate runs of 6 replicates each for all QC samples. Relative standard deviations were calculated for precisions. Dilution integrity was tested on one day (n = 6) by diluting 10 µl of 4000 ng/ml plasma repotrectinib QC sample with 90 µl blank human plasma (1:10 dilution) before further treatment of 10 µl of diluted mixture.

Table 2
Assay performance data (n = 18, 3 days) of repotrectinib in mouse plasma.

Level (ng/ml)	Intra-day precision (%)	Inter-day precison (%)	Accuracy (%)
750	1.4	3.2	99.1
50	1.3	2.2	104.9
2.5	3.5	4.7	104.3
1	8.4	8.7	106.4

Table 3
Assay performance data (n = 18, 3 days) and stability (recovery after 6 h storage at ambient temperature) of 50 ng/ml repotrectinib in tissue homogenates.

Tissue	Intra-day precision (%)	Inter-day precision (%)	Accuracy (%)	Recovery (%)
Brain	2.9	3.1	100.3	98.3 ± 1.6
Kidney	1.9	2.8	105.3	90.1 ± 1.6
Liver	2.0	3.0	103.9	99.1 ± 2.1
Small intestinal tissue	3.6	5.4	107.3	102.7 ± 4.6
Small intestinal content	3.8	5.0	90.5	95.9 ± 5.2
Spleen	2.0	2.9	101.1	95.0 ± 1.7
Testis	1.8	2.8	102.6	93.2 ± 1.2

2.8.5. Drug stability

The stability of repotrectinib was investigated in mouse plasma at QC-high and QC-low levels (all n = 6). The separate portions of 10 µl in 200 µl well plates were kept under different conditions, including ambient temperature (ca. 20 °C) for 24 h, three additional freeze-thaw cycles (thawing at room temperature for 1 h, and freeze again at least for one day at −30 °C), and −30 °C for 2.5 months. Stability of repotrectinib in pooled brain, liver, spleen, kidney, small intestinal tissue, small intestinal content, and testis homogenate was studied at QC-medium level at ambient temperature for 6 h. A complete validation run with diluted extracts of calibration and 24 QC samples was analyzed after 7 days storage at 4 °C to test the stability of repotrectinib in the autosampler.

2.9. Pharmacokinetic and tissue distribution of repotrectinib

2.9.1. Mouse experiment

A repotrectinib pharmacokinetic study was performed in wild-type female mice (FVB/NRj genetic background) by oral administration of 10 mg/kg repotrectinib (n = 6). Repotrectinib was dissolved in dimethyl sulfoxide (50 mg/ml), followed by 3-fold dilution with polysorbate 80/ethanol (1/1; v/v), and then further diluted with a 10 mM hydrochloric acid solution to obtain a dose solution of 1 mg/ml, freshly prepared on the experimental day. The experiment animal protocol was evaluated and approved in the Netherlands Cancer Institute by the institutional animal care and use committee. According to institutional guidelines complying with Dutch legislation, mice were 11–12 weeks of age and kept in a temperature-controlled environment with a 12-h light and 12-h dark cycle and they received a standard diet and acidified water *ad libitum*. Repotrectinib (10 mg/kg) was administered to mice by oral gavage, with a blunt-end needle, after 2–3 h fasting. Serial tail vein blooding sampling were performed at 7.5, 15, 30 min and 1, 2, and 4 h time point. Eight hours after oral administration, blood samples were collected by cardiac puncture when the mice were under anesthesia with isoflurane. After sacrificing mice by cervical dislocation, brain, liver, spleen, kidney, small intestinal tissue, and small intestinal content were rapidly harvested, weighed, and homogenized as described in Section 2.2. Plasma was isolated from blood by centrifugation at 9000*g* for 6 min at 4 °C and was stored at −30 °C until analysis. Mouse plasma samples were diluted by 10-fold with human lithium heparin plasma for further sample preparation and analysis.

2.9.2. Pharmacokinetic calculations

Pharmacokinetic parameters were calculated in Microsoft Excel using the first-order one-compartment model. The peak plasma concentration (C_{max}) and the time to reach the maximum plasma concentration (t_{max}) were assessed from highest plasma concentration of each individual mouse. The area under the plasma concentration-time curve during the 8-h experiment ($AUC_{0\rightarrow8}$) and the extrapolated value ($AUC_{0\rightarrow\infty}$) were calculated using the trapezoidal rule and extrapolation from 8 h to infinity using the elimination rate and the concentration at 8 h. The half-life ($t_{1/2}$), apparent clearance (Cl/F), as well as apparent volume of distribution (Vd/F) were also calculated.

2.9.3. Incurred samples reanalysis

To demonstrate assay reproducibility, 42 incurred (study) samples were reanalyzed. Six diluted plasma and 36 tissue homogenate samples, 6 of each tissue, were reanalyzed within a few days.

3. Results and discussion

3.1. Method development

Protein precipitation as sample preparation method followed by LC-MS/MS has been applied in several bioanalysis methods for many tyrosine kinase inhibitors [11–13]. This procedure was also adopted in this assay because it is simpler, less expensive, and less time-consuming compared to other extraction methods, such as liquid-liquid extraction (LLE) and solid phase extraction (SPE). Acetonitrile, as a precipitant agent, was selected to yield significantly higher response of the tested compounds than methanol and ethanol (data not shown). 25% (v/v) methanol in water was added to the extract to obtain symmetric and sharp peaks because the eluent contained less organic modifier than the extract. Moreover, an appropriate injection volume and reduced MS response to avoid saturation of the electron multiplier can be achieved by sample dilution.

Since a stable isotopically labeled analogue of repotrectinib was not commercially available, seventeen compounds were screened and three different drugs eluting at similar retention times were investigated as potential internal standards during method development. Axitinib showed better precisions and accuracies compared to erlotinib and momelotinib and was therefore selected as IS for the complete analytical method validation. Because axitinib undergoes light induced isomerization, it shows two non-separated chromatograph peaks (Fig. 2B). To obtain a constant ratio of two isomers, axitinib was already exposed to light before used as IS [14]. The quantification of axitinib included both isomers to achieve consistent signal in this assay. Any metabolites of repotrectinib were unknown during our study and were therefore not considered to be included in this assay.

Chromatographic retention was optimized on the column to obtain short runs but sufficient retention to circumvent matrix effects. The combination of methanol and 0.1% ammonium hydroxide was selected due to better peak shape and signal-to-noise ratios compared to acetonitrile and formic acid or acetic acid. After optimization of chromatographic conditions, SRM in positive mode was optimized for protonated ions at *m/z* 356.1 for repotrectinib and *m/z* 387.1 for axitinib, respectively. A product spectrum of repotrectinib is shown in Fig. 1 with the proposed fragmentation product. A product spectrum of axitinib was reported previously by us [14].

3.2. Method validation

Based on pharmacokinetic parameters from patients [8] and the LC-MS/MS response, the calibration curve range (1–1000 ng/ml) was selected. Dilution integrity was included in the validation program to quantify the levels exceeding this range. Representative chromatograms of repotrectinib and axitinib in mouse plasma are shown in Fig. 2.

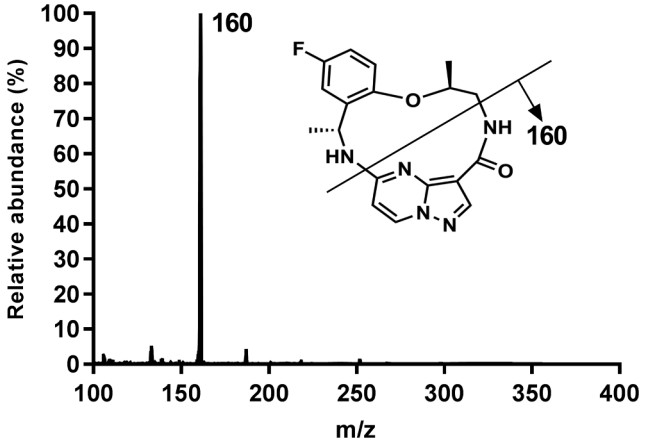

Fig. 1. Chemical structure and product spectrum (*m/z* 356.1@73 V) of the protonated molecule of repotrectinib ($[M + H]^+$) with the expected fragments.

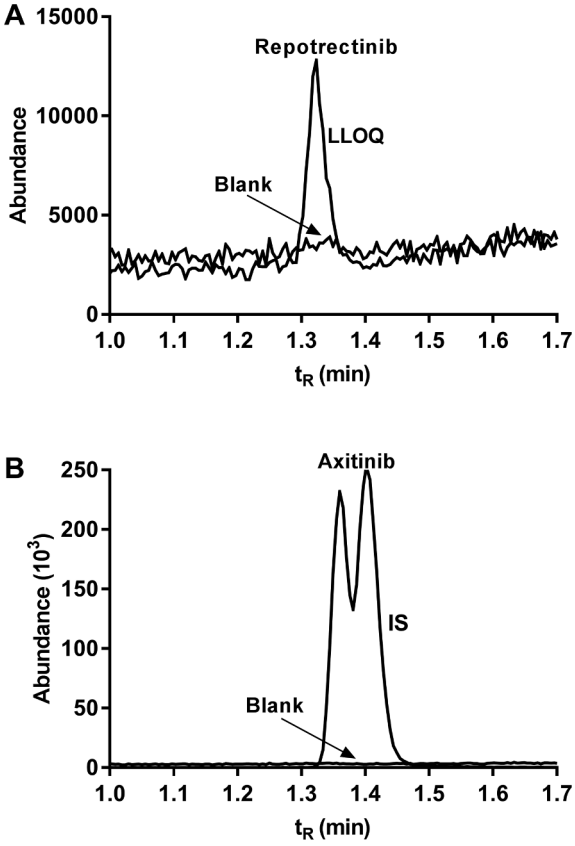

Fig. 2. SRM chromatograms of a blank pooled plasma sample and a LLOQ spiked sample. (A) repotrectinib (*m/z* 356.1 → 160.0 @73 V) and (B) axitinib (*m/z* 387.1 → 356.0 @29 V) in mouse plasma.

3.2.1. Selectivity

There were no potentially interfering peaks for repotrectinib or IS in double blank and blank mouse plasma and tissue homogenate samples (n = 34). Blank axitinib responses did not exceed 1.5% of the normal IS response. Moreover, concentrations calculated at the LLOQ spiked plasma (n = 6) and tissue homogenates (n = 28) were 1.033 ± 0.071 ng/ml and 0.947 ± 0.097 ng/ml, respectively, with only two small intestinal content samples exceeding 120% of target value.

3.2.2. Recovery and matrix effect

The recovery (100.3 ± 10.3, 107.8 ± 6.2%, 108.2 ± 5.5%) and

matrix effect (99.7 ± 3.1%, 91.4 ± 2.4%, 96.8 ± 7.0%) in plasma at high, medium and low repotrectinib QC levels were good (n = 6) and indicating that no significant extraction losses or matrix effect occurred. Because the matrix effect and recovery of repotrectinib and IS in tissue homogenates are similar to those in plasma, plasma was used as surrogate matrix for analysis of tissue samples. The relative matrix effect in individual tissue homogenates (n = 28) also showed results (96.1 ± 1.8% and 91.1 ± 2.9% at high and low QCs) (Supplemental Table 1) without significant matrix effects.

3.2.3. Calibration

Least-squares quadratic (second degree polynomial) regression was adopted instead of linear regression due to non-linearity relative response of repotrectinib at higher concentrations (Supplemental Table 2), probably due to saturation of the electron multiplier. The calibration results were given as quadratic model ($y = A + B{\cdot}x + C{\cdot}x^2$) with parameters A (intercept), B (slope), and C (quadratic factor), the coefficient of determination (R^2) and y being target peak area relative to IS and × the repotrectinib concentration in ng/ml. Calibration parameters are reported as mean ± SD (n = 10). The average equation obtained was $y = 8.97\ (\pm 6.74) \cdot 10^{-4} + 13.54\ (\pm 0.64) \cdot 10^{-3}{\cdot}x - 1.84\ (\pm 0.80){\cdot}10^{-6}{\cdot}x^2$ with $R^2 = 0.998\ (\pm 0.0014)$.

3.2.4. Precision and accuracy

Assay performance data of QC samples were investigated at four levels for plasma samples and medium level for each tissue homogenate. As shown in Tables 2 and 3, the intra- and inter-assay precision, and accuracy results at all levels and matrices were within ± 15% for high, medium, and low QCs and within ± 20% for LLOQ as required [9,10]. For dilution integrity at 4000 ng/ml (n = 6) precision was 2.1% and accuracy was 89%, meeting the same ± 15% requirement.

3.2.5. Stability

The stability of repotrectinib in lithium heparin mouse plasma and pooled tissue homogenates is presented in Tables 4 and 3, respectively. The data suggest that no significant degradation of repotrectinib was observed in all tested matrices under all tested conditions. Moreover, measuring a complete analytical run after 7 days at 4 °C resulted in a successful performance (98.1 ± 2.3%, 102.8 ± 1.5%, 103.8 ± 2.7%, and 105.9 ± 6.1% for high-, medium-, low-QC, and LLOQ, respectively) without any QC sample (n = 24) exceeding ± 15%.

3.3. Pharmacokinetic study of repotrectinib in mice

This method was successfully used for the analysis of samples from a pharmacokinetic study of repotrectinib.

3.3.1. Plasma pharmacokinetics

The average plasma concentration-time curve of repotrectinib in wild-type mice (FVB/NRj background, n = 6) after oral administration of 10 mg/kg repotrectinib is shown in Fig. 4A, a representative chromatogram is shown in Fig. 3A. The calculated pharmacokinetic parameters of repotrectinib were: C_{max} = 4803 ± 1778 ng/ml, T_{max} = 0.54 ± 0.25 h, $T_{1/2}$ = 1.49 ± 0.46 h, $AUC_{0\rightarrow 8}$ = 16277 ± 6350 ng·h·ml^{-1}, $AUC_{0\rightarrow\infty}$ = 19609 ± 7055 ng·h·ml^{-1}, Cl/F = 558 ± 166 ml·h^{-1}·kg^{-1}, and V_d/F = 1242 ± 628 ml/kg.

Table 4
Stability data (recovery [%]; ± S.D.; n = 6) of repotrectinib in mouse plasma, reporting the percentage of the initial concentration.

Condition	QC-high	QC-low
3 freeze-thaw cycles	96.8 ± 1.5	101.1 ± 3.6
24 h at ambient temperature	93.6 ± 2.8	101.0 ± 2.6
2.5 months at −30 °C	101.5 ± 2.9	103.3 ± 3.5

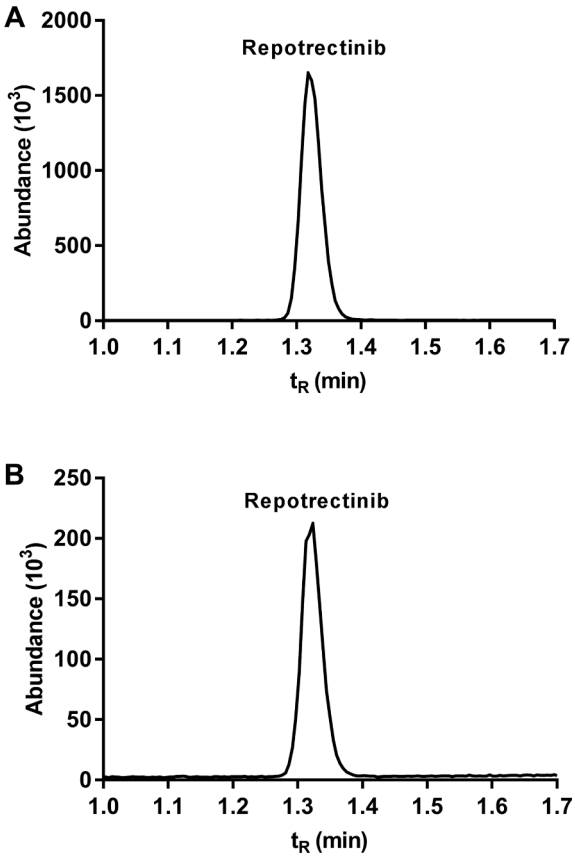

Fig. 3. SRM chromatograms (*m/z* 356.1 → 160.0 @73 V) of repotrectinib in (A) 4-h plasma (561 ng/ml) and (B) 8-h brain homogenate (34.9 ng/ml) after oral administration of 10 mg/kg to a FVB/NRj mouse.

3.3.2. Tissue distribution

Repotrectinib was also quantified in tissue homogenates, and drug concentrations (ng/g) in tissues were calculated considering the total weight of each organ and the solvent. The weight of brain, kidney, liver, small intestine, small intestinal content, and spleen was around 0.41, 0.29, 1.11, 0.75, 0.33, and 0.10 g, respectively. The relative tissue distribution of repotrectinib at 8 h after oral administration is shown in Fig. 4B and a chromatogram of the drug in brain homogenate is shown in Fig. 3B. Repotrectinib is highly distributed in small intestinal content, small intestine and liver, followed by kidney, spleen, and brain. These data indicate that repotrectinib is relatively poorly penetrated into the brain, probably due to the blood-brain barrier, where multispecific drug efflux transporters, like P-glycoprotein and breast cancer resistance protein are abundantly expressed. One or more of these efflux transporters might actively pump repotrectinib out from the brain to plasma, leading to the low brain distribution of repotrectinib. Moreover, compared to the brain-to-plasma ratios of lorlatinib at 8 h (0.46) [15], a macrocyclic third-generation ALK inhibitor, repotrectinib showed less capacity of penetration into brain even with a small molecular weight.

3.3.3. Incurred samples reanalysis

All the results of reanalysed samples (n = 42), including plasma and tissue homogenates, are within ± 20%, suggesting an excellent success rate not exceeding the 33% of the guidelines [9,10] by far.

4. Conclusions

To the best of our knowledge, this is the first reported and

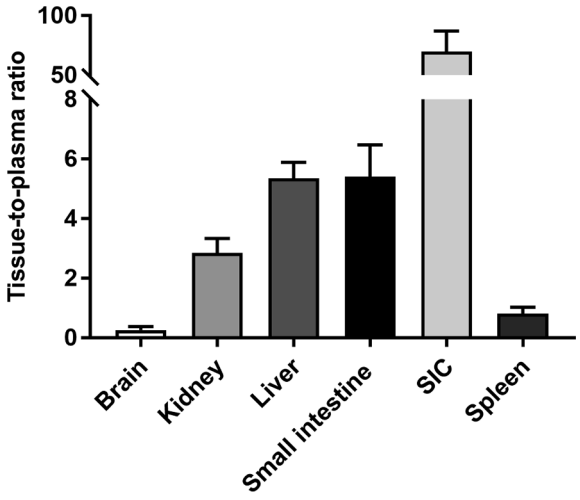

Fig. 4. Plasma concentration-time curve (A) and tissue-to-plasma ratios (B) in female FVB/NRj mice (n = 6) in 6 tissues, 8 h after oral administration of 10 mg/kg repotrectinib.

successfully validated bioanalytical assay developed for repotrectinib, a next-generation ROS1/TRK/ALK inhibitor, in only 10 µl plasma or tissue homogenate. Moreover, this LC-MS/MS method was successfully adopted to study the pharmacokinetics and tissue distribution of repotrectinib in mice due to the small sample volume used and might be further applied in clinical studies in the future.

CRediT authorship contribution statement

Wenlong Li: Conceptualization, Methodology, Investigation, Data curation, Writing - original draft. **Nikoletta Perpinioti:** Conceptualization, Methodology, Investigation. **Alfred H. Schinkel:** Writing - review & editing. **Jos H. Beijnen:** Writing - review & editing. **Rolf W. Sparidans:** Conceptualization, Supervision, Writing - review & editing.

Declaration of Competing Interest

The authors declare that they have no known competing financial interests or personal relationships that could have appeared to influence the work reported in this paper.

Acknowledgement

This work was funded in part by the China Scholarship Council (CSC Scholarship No. 201606220081 to Wenlong Li).

Appendix A. Supplementary material

Supplementary data to this article can be found online at https://doi.org/10.1016/j.jchromb.2020.122098.

References

[1] J.J. Lin, A.T. Shaw, Recent advances in targeting ROS1 in lung cancer, J. Thoracic Oncol.: Off. Publ. Int. Assoc. Study Lung Cancer 12 (2017) 1611–1625.
[2] E. Grande, M.V. Bolos, E. Arriola, Targeting oncogenic ALK: a promising strategy for cancer treatment, Mol. Cancer Ther. 10 (2011) 569–579.
[3] S.H. Ou, J. Tan, Y. Yen, R.A. Soo, ROS1 as a 'druggable' receptor tyrosine kinase: lessons learned from inhibiting the ALK pathway, Expert Rev. Anticancer Ther. 12 (2012) 447–456.
[4] S.I. Ou, V.W. Zhu, CNS metastasis in ROS1+ NSCLC: An urgent call to action, to understand, and to overcome, Lung cancer (Amsterdam, Netherlands) 130 (2019) 201–207.
[5] E. Cocco, M. Scaltriti, A. Drilon, NTRK fusion-positive cancers and TRK inhibitor therapy, Nat. Rev. Clin. Oncol. 15 (2018) 731–747.
[6] A. Drilon, T.W. Laetsch, S. Kummar, S.G. DuBois, U.N. Lassen, G.D. Demetri, M. Nathenson, R.C. Doebele, A.F. Farago, A.S. Pappo, B. Turpin, A. Dowlati, M.S. Brose, L. Mascarenhas, N. Federman, J. Berlin, W.S. El-Deiry, C. Baik, J. Deeken, V. Boni, R. Nagasubramanian, M. Taylor, E.R. Rudzinski, F. Meric-Bernstam, D.P.S. Sohal, P.C. Ma, L.E. Raez, J.F. Hechtman, R. Benayed, M. Ladanyi, B.B. Tuch, K. Ebata, S. Cruickshank, N.C. Ku, M.C. Cox, D.S. Hawkins, D.S. Hong, D.M. Hyman, Efficacy of Larotrectinib in TRK fusion-positive cancers in adults and children, New England J. Med. 378 (2018) 731–739.
[7] A. Drilon, S. Siena, S.I. Ou, M. Patel, M.J. Ahn, J. Lee, T.M. Bauer, A.F. Farago, J.J. Wheler, S.V. Liu, R. Doebele, L. Giannetta, G. Cerea, G. Marrapese, M. Schirru, A. Amatu, K. Bencardino, L. Palmeri, A. Sartore-Bianchi, A. Vanzulli, S. Cresta, S. Damian, M. Duca, E. Ardini, G. Li, J. Christiansen, K. Kowalski, A.D. Johnson, R. Patel, D. Luo, E. Chow-Maneval, Z. Hornby, P.S. Multani, A.T. Shaw, F.G. De Braud, Safety and Antitumor Activity of the Multitargeted Pan-TRK, ROS1, and ALK Inhibitor Entrectinib: Combined Results from Two Phase I Trials (ALKA-372-001 and STARTRK-1), Cancer Discov. 7 (2017) 400–409.
[8] A. Drilon, S.I. Ou, B.C. Cho, D.W. Kim, J. Lee, J.J. Lin, V.W. Zhu, M.J. Ahn, D.R. Camidge, J. Nguyen, D. Zhai, W. Deng, Z. Huang, E. Rogers, J. Liu, J. Whitten, J.K. Lim, S. Stopatschinskaja, D.M. Hyman, R.C. Doebele, J.J. Cui, A.T. Shaw, Repotrectinib (TPX-0005) Is a Next-Generation ROS1/TRK/ALK Inhibitor That Potently Inhibits ROS1/TRK/ALK Solvent- Front Mutations, Cancer Discov. 8 (2018) 1227–1236.
[9] European Medicines Agency, www.ema.europa.eu/ema/pages/includes/document/open_document.jsp?webContentId=WC500109686, 2011, Accessed: August 1, 2018, DOI.
[10] Center for Drug Evaluation and Research of the U.S. Department of Health and Human Services Food and Drug Administration, 2018, http://www.fda.gov/Drugs/GuidanceComplianceRegulatoryInformation/Guidances/ucm064964.htm, Accessed: August 2, 2018., DOI.
[11] C. Spatari, W. Li, A.H. Schinkel, G. Ragno, J.H.M. Schellens, J.H. Beijnen, R.W. Sparidans, Bioanalytical assay for the quantification of the ALK inhibitor lorlatinib in mouse plasma using liquid chromatography-tandem mass spectrometry, J. Chromatogr. B, Anal. Technol. Biomed. Life Sci. 1083 (2018) 204–208.
[12] B. Dogan-Topal, W. Li, A.H. Schinkel, J.H. Beijnen, R.W. Sparidans, Quantification of FGFR4 inhibitor BLU-554 in mouse plasma and tissue homogenates using liquid chromatography-tandem mass spectrometry, J. Chromatogr. B, Anal. Technol. Biomed. Life Sci. 1110–1111 (2019) 116–123.
[13] J.J.M. Rood, J.H.M. Schellens, J.H. Beijnen, R.W. Sparidans, Recent developments in the chromatographic bioanalysis of approved kinase inhibitor drugs in oncology, J. Pharm. Biomed. Anal. 130 (2016) 244–263.
[14] R.W. Sparidans, D. Iusuf, A.H. Schinkel, J.H. Schellens, J.H. Beijnen, Liquid chromatography-tandem mass spectrometric assay for the light sensitive tyrosine kinase inhibitor axitinib in human plasma, J. Chromatogr. B, Anal. Technol. Biomed. Life Sci. 877 (2009) 4090–4096.
[15] W. Li, R.W. Sparidans, Y. Wang, M.C. Lebre, E. Wagenaar, J.H. Beijnen, A.H. Schinkel, P-glycoprotein (MDR1/ABCB1) restricts brain accumulation and cytochrome P450–3A (CYP3A) limits oral availability of the novel ALK/ROS1 inhibitor lorlatinib, Int. J. Cancer 143 (2018) 2029–2038.